Self-Assembly of Rod−Coil Molecules into Molecular Length-Dependent Organization

Ja-Hyoung Ryu,[†] Nam-Keun Oh,[‡] Wang-Cheol Zin,[‡] and Myongsoo Lee*,[†]

Contribution from the Center for Supramolecular Nano-Assembly and Department of Chemistry, and Yonsei University, Seoul 120-749, Korea, and Department of Materials Science & Engineering, Pohang University of Science and Technology, Pohang 790-784, Korea

Received November 25, 2003; E-mail: mslee@yonsei.ac.kr

Abstract: A series of rod−coil molecules (**n−x**, where **n** represents the number of repeating units in a PPO coil and **x** the number of phenyl groups in a rod segment) with variation in the molecular length, but an identical rod to coil volume ratio was synthesized, and their self-assembling behavior was investigated by using DSC and X-ray scatterings. The molecule with a short rod−coil molecule (**16−4**) shows a 3-D tetragonal structure based on a body-centered symmetry of the discrete bundles in addition to a lamellar structure. This 3-D lattice, on heating, collapses to generate a disordered micellar structure. Remarkably, the molecules based on longer molecular length (**21−5** and **24−6**) were observed to self-organize into, on heating, lamellar, tetagonally perforated lamellar, 2-D hexagonal columnar and finally disordered micellar structures. Further increase in the molecular length as in the case of **29−7** and **32−8** induces a 3-D hexagonally perforated lamellar structure as an intermediate structure between the lamellar and tetragonally perforated lamellar structures. Consequently, these systems demonstrate the ability to regulate the domain nanostructure, from 2-dimensionally continuous layers, long strips to discrete bundles via periodic perforated layers by small changes in the molecular length, at an identical rod-to-coil volume fraction.

Introduction

One of the great challenges in supramolecular chemistry is the development of individual molecular units that are capable of organizing into ordered states through weak intermolecular forces, such as hydrogen bonding, donor−acceptor interactions, repulsive interactions, and reversible ligand−metal interactions.[1] Self-assembling molecules, which include liquid-crystals,[2] block copolymers,[3,4] hydrogen bonded complexes,[5,6] and coordination polymers[7−9] are widely studied for their great potential as advanced functional materials. Among synthetic self-organizing systems, rod−coil molecules are of particular interest because of the potential of incorporating desirable chemical functionality and physical properties at nanoscale dimensions as well as many advantages associated with short chain lengths of the respective blocks.[10] The aggregation architecture and the properties can

be tuned by careful selection of the type and relative length of the respective blocks.[11−16] Previous publications from our laboratory reported synthesis and structural analysis of rod−coil block systems that self-assemble into lamellar, cylindrical, and discrete nanostructures depending on the relative volume fraction of the rod segments (Figure 1).[17] In addition, we have demonstrated that the supramolecular structure can be controlled by varying the number of grafting sites per rod.[18] The shape

† Yonsei University.

‡ Pohang University of Science and Technology.

(1) Lehn, J. M. *Supramolecular Chemistry, Concepts and Perspective*; VCH: Weinheim, Germany, 1995.

(2) (a) Collings, P. J.; Hird, M. *Introduction to Liquid Crystals, Chemistry and Physics*; Taylor & Francis Ltd: London, UK, 1997. (b) Tschierske, C. *J. Mater. Chem.* **2001**, *11*, 2647−2671.

(3) (a) Förster, S.; Plantenberg, T. *Angew. Chem., Int. Ed.* **2002**, *41*, 688−714. (b) Förster, S.; Antonietti, M. *Adv. Mater.* **1998**, *10*, 195−217.

(4) Khandpur, A. K.; Förster, S.; Bates, F. S.; Hamley, I. W.; Ryan, A. J.; Bras, W.; Almdal, K.; Mortensen, K. *Macromolecules* **1995**, *28*, 8796−8806.

(5) Zeng, F.; Zimmerman, S. C. *Chem. Rev.* **1997**, *97*, 1681−1712.

(6) Brunsveld, L.; Folmer, B. J. B.; Meijer, E. W.; Sijbesma, R. P. *Chem. Rev.* **2001**, *101*, 4071−4097.

(7) Hennigar, T. L.; MacQuarrie, D. C.; Losier, P.; Rogers, R. D.; Zaworotko, M. J. *Angew. Chem., Int. Ed. Engl.* **1997**, *36*, 972−973.

(8) Kaes, C.; Hosseini, M. W.; Rickard, C. E. F.; Skelton, B. W.; White, A. H. *Angew. Chem., Int. Ed. Engl.* **1998**, *37*, 920−922.

(9) Cui, Y.; Lee, S. J.; Lin, W. *J. Am. Chem. Soc.* **2003**, *125*, 6014−6015.

(10) Recent Reviews: (a) Lee, M.; Yoo, Y.-S. *J. Mater. Chem.* **2002**, *12*, 2161−2168. (b) Lee, M.; Cho, B.-K.; Zin, W.-C. *Chem. Rev.* **2001**, *101*, 3869−3892. (c) Klok, H.-A.; Lecommandoux, S. *Adv. Mater.* **2001**, *13*, 1217−1229. (d) Stupp, S. I. *Curr. Opin. Colloid Interface Sci.* **1998**, *3*, 20−26. (e) Loos, K.; Munoz-Guerra, S. *Supramolecular Polymers-Chapter 7: Microstructure and Crystallization of Rigid-Coil Comblike Polymers and Block Copolymers*; Marcel Dekker: New York, 2000.

(11) Cornelissen, J. J. L. M.; Fischer, M.; Sommerdijk, N. A. J. M.; Nolte, R. J. M. *Science* **1998**, *280*, 1427−1430.

(12) Jenekhe, S. A.; Chen, X. L. *Science* **1999**, *283*, 372−375.

(13) (a) Stupp, S. I.; LeBonheur, V.; Walker, K.; Li, L. S.; Huggins, K. E.; Keser, M.; Amstutz, A. *Science* **1997**, *276*, 384−389. (b) Radzilowski, L. H.; Carragher, B. O.; Stupp, S. I. *Macromolecules* **1997**, *30*, 2110−2119.

(14) Chen, J. T.; Thomas, E. L.; Ober, C. K.; Mao, G. S*cience* **1996**, *273*, 343−346.

(15) Tu, Y.; Wan, X.; Zhang, H.; Fan, X.; Chen, X.; Zhou, Q.-F.; Chau, K. *Macromolecules* **2003**, *36*, 6565−6569.

(16) Vriezema, D. M.; Hoogboom, J.; Velonia, K.; Takazawa, K.; Christianen, P. C. M.; Maan, J. C.; Rowan, A. E.; Nolte, R. J. M. *Angew. Chem., Int. Ed.* **2003**, *42*, 772−776.

(17) (a) Lee, M.; Cho, B.-K.; Kim, H.; Zin, W.-C. *Angew. Chem., Int. Ed.* **1998**, *37*, 638−640. (b) Lee, M.; Cho, B.-K.; Kim, H.; Yoon, J.-Y.; Zin, W.-C. *J. Am. Chem. Soc.* **1998**, *120*, 9168−9179. (c) Lee, M.; Lee, D.-W.; Cho, B.-K.; Yoon, J.-Y.; Zin, W.-C. *J. Am. Chem. Soc.* **1998**, *120*, 13258−13259. (d) Lee, M.; Cho, B.-K.; Kang, Y.-S.; Zin, W.-C. *Macromolecules* **1999**, *32*, 7688−7691. (e) Lee, M.; Cho, B.-K.; Kang, Y.-S.; Zin, W.-C. *Macromolecules* **1999**, *32*, 8531−8537.

(18) Lee, M.; Cho, B.-K.; Oh, N.-K.; Zin, W.-C. *Macromolecules* **2001**, *34*, 1987−1995.

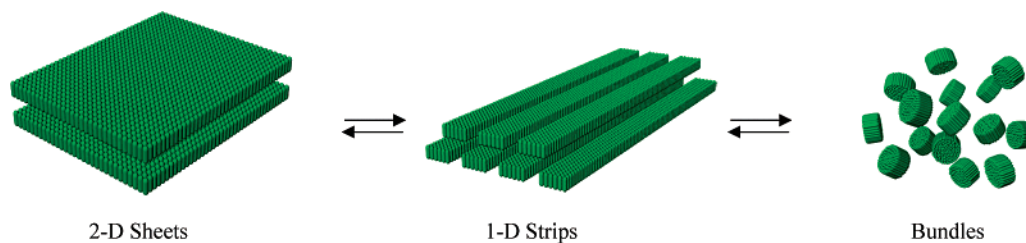2-D Sheets   1-D Strips   Bundles

Figure 1. Schematic representation illustrating the nanostructures formed through self-assembly of rod building blocks in rod−coil systems. Stiff rod building blocks have a strong tendency to assembly into a sheetlike organization. With increasing coil volume fraction, however, 2-D sheetlike rod domains split successively into 1-D striplike domains and discrete objects, possibly to minimize energy associated with coil stretching.

and size of the aggregation structure have also been reported to have a strong influence on the photophysical properties of the materials.[19]

We have previously shown that rod−coil systems with an elongated rod block self-assemble into discrete bundles or perforated layers that organize into a 3-D superlattice.[20] In a preliminary communication, we also demonstrated that the variation of the rod length at the constant rod to coil volume ratio leads to structural inversion from discrete nanostructures to continuous rod layers.[21] These results imply that the length of the rod building blocks as well as volume ratio between the blocks in rod−coil systems has a strong influence on the shape of the supramolecular structure. The strong tendency of the rod building blocks to be arranged into anisotropic crystalline order along their axes seems to play a crucial role in the formation of controlled supramolecular structures. However, apparent elucidation of the architectural influence on the supramolecular structure requires the synthesis of the rod−coil molecules with systematic variation in the rod length at the identical rod to coil volume ratio. In this context, we have synthesized a series of structurally simple rod−coil diblock molecules based on a poly(propylene oxide) (PPO) coil with variation in the molecular length, but an identical rod to coil volume ratio and investigated their self-assembling behavior in the solid state.

In this article, we describe the synthesis of a series of rod−coil diblock molecules (**n−x**, where **n** represents the number of repeating units in a PPO coil and **x** the number of phenyl groups in a rod segment) and their self-assembling behavior characterized by optical polarized microscopy, differential scanning calorimetry and powder X-ray diffraction measurements. Since the rod−coil molecules are all based on identical rod to coil volume ratio ($f_{rod} = 0.23$), the supramolecular structural variation can mainly be attributed to the variation of molecular length. With increasing the molecular length at an identical rod to coil volume ratio, the rod building blocks self-assemble into successively discrete bundles, long strips, tetragonally perforated layer, hexagonally perforated layer and finally conventional layers. Consequently, the key feature of this system is the ability to generate complicated but systematic structural transformation with simple variation in the molecular length.
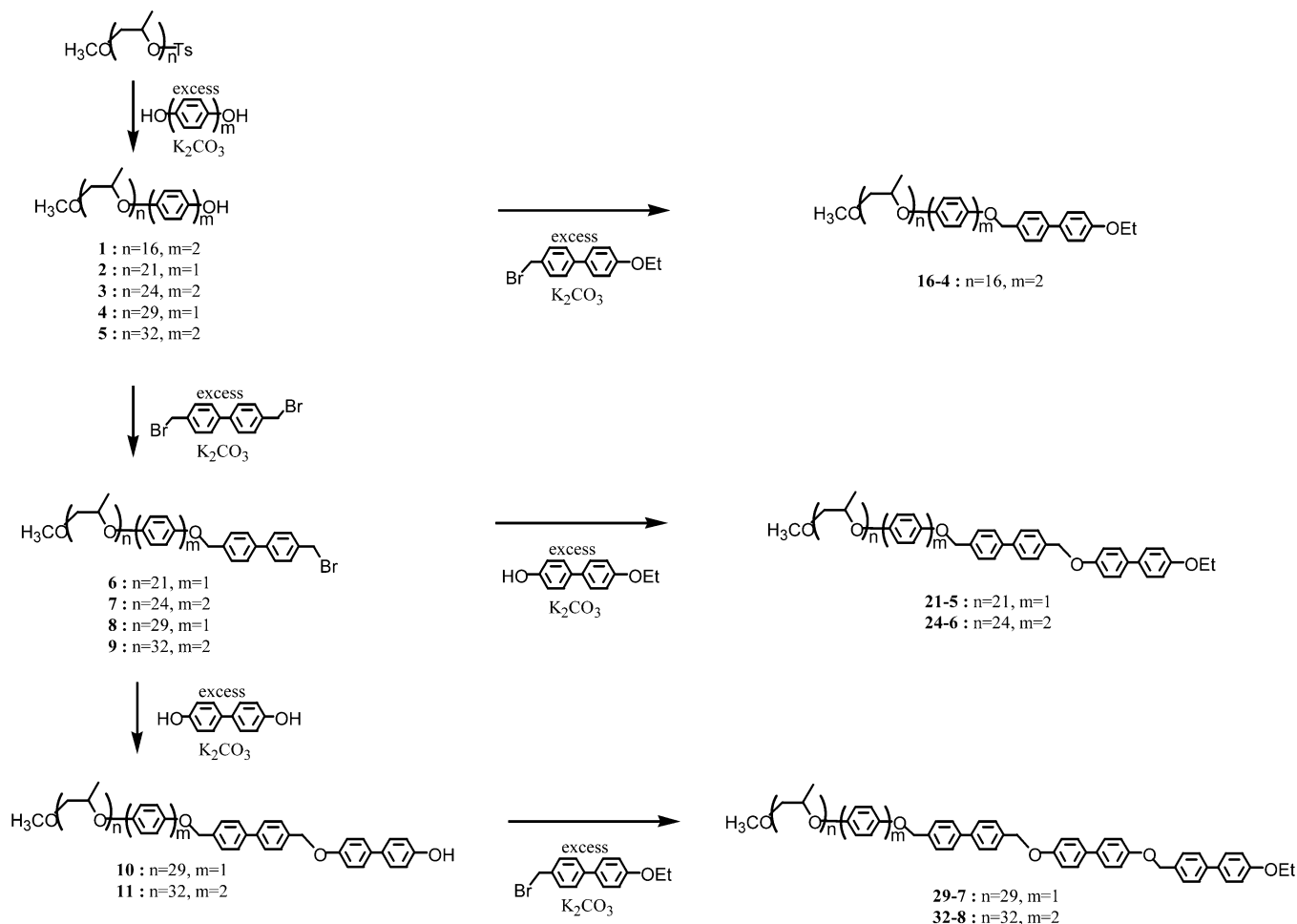
(19) (a) Lee, M.; Kim, J.-W.; Hwang, I.-W.; Kim. Y.-R.; Oh, N.-K.; Zin, W.-C. *Adv. Mater.* **2001**, *13*, 1363−1368. (b) Lee, M.; Jeong, Y.-S.; Cho, B.-K.; Oh, N.-K.; Zin, W.-C. *Chem. Eur. J.* **2002**, *8*, 876−883.
(20) (a) Lee, M.; Cho, B.-K.; Jang, Y.-G.; Zin, W.-C. *J. Am. Chem. Soc.* **2000**, *122*, 7449−7455. (b) Lee, M.; Cho, B.-K.; Ihn, K. J.; Lee, W.-K.; Oh. N.-K.; Zin, W.-C. *J. Am. Chem. Soc.* **2001**, *123*, 4647−4648.
(21) Cho, B.-K.; Lee, M.; Oh, N.-K.; Zin, W.-C. *J. Am. Chem. Soc.* **2001**, *123*, 9677−9678.

Results and Discussion

Synthesis. The synthesis of rod−coil molecules consisting of poly(propylene oxide) as a coil segment and aromatic units connected by methylene ether linkages as a rod building block is outlined in Scheme 1 and start with the preparation of tosylated poly(propylene oxide) coils with the appropriate number of propylene oxide repeating units.[17b] Monophenol terminated or monophenylphenol terminated poly(propylene oxide)s **1−5** were prepared from the reaction of of the appropriate tosylated poly(propylene oxide) with an excess amount of hydroquinone or 4,4′-biphenol. Rod-coil molecule **16−4** was synthesized by etherification of **1** with 4-bromethyl-4′-ethoxy biphenyl in the presence of potassium carbonate. Etherification of **2** with an excess of 4,4′-dibromomethyl biphenyl and subsequent reaction with 4-hydroxy-4′-ethoxy biphenyl produced **21−5**. Rod-coil molecule **24−6** was obtained by following the same sequence of reactions, i.e., by etherification of **3** with an excess of 4,4′-dibromomethyl biphenyl and subsequent etherification with 4-hydroxy-4′-ethoxy biphenyl. Both **29−7** and **32−8** based on the longest chain length in this series was prepared from the reaction of **8** and **9**, respectively, with an excess of 4,4′-biphenol and subsequent reaction with 4-bromethyl-4′-ethoxy biphenyl.

All of the resulting rod−coil molecules were purified silica gel column chromatography and then prep-HPLC until transition temperature and polydispersity index remained constant as described in the Experimental Section. The rod−coil molecules were characterized by ¹H NMR spectroscopy, elemental analysis and gel permeation chromatography (GPC) and shown to be in full agreement with the expected chemical structures. All of the rod−coil molecules showed a very narrow molecular weight distribution with polydispersity index of less than 1.06, as determined from GPC (Table 1). As confirmed by ¹H NMR spectroscopy, the number of repeating units in the coil segment determined from the ratio of the benzyl protons of the rod block to the ethylene protons of poly(propylene oxide) was in good agreement with the expected value. Therefore, these rod−coil molecules with different rod lengths represent to have the same rod volume fraction relative to coil segment ($f_{rod} = 0.23$).

Structural Investigation. The self-assembling behavior of the rod−coil molecules was investigated by means of differential scanning calorimetry (DSC), thermal optical polarized microscopy and X-ray scatterings. Figure 2 presents the DSC heating and cooling traces of the rod−coil molecules. All of the molecules show an ordered bulk-state structure that is thermodynamically stable, as verified by the heating and cooling DSC scans. The transition temperatures and the corresponding enthalpy changes determined from DSC heating and cooling

Scheme 1. Synthesis of Rod-Coil Molecules

1 : n=16, m=2
2 : n=21, m=1
3 : n=24, m=2
4 : n=29, m=1
5 : n=32, m=2

16-4 : n=16, m=2

6 : n=21, m=1
7 : n=24, m=2
8 : n=29, m=1
9 : n=32, m=2

21-5 : n=21, m=1
24-6 : n=24, m=2

10 : n=29, m=1
11 : n=32, m=2

29-7 : n=29, m=1
32-8 : n=32, m=2

Table 1. Thermal Transitions of Rod−Coil Molecules $n-x$ (data are from heating and cooling scans)[a]

rod-coil molecules	coil DP[b]	M_w/M_n[c]	phase transition (°C) & corresponding enthalpy changes (kJ/mol)	
			heating	cooling
16−4	16.3	1.05	L 84.1 (9.3) M_{tet} 100.7 (3.5) M 105.8 (3.8) i	i 103.5 (3.8) M 97.5 (3.5) M_{tet} 66.4 (11.2) L
21−5	21.3	1.05	L 71.6 (8.1) L_{tet} 109.3 (0.6) col 141.2 (4.1) M 165.8 (5.6) i	i 159.0 (5.7) M 134.2 (4.0) col 64.1 (0.6) L_{tet}
24−6	24.4	1.03	L 111.0 (9.9) L_{tet} 201.5 (8.2) col 215.0 (3.1) M 234.0 (7.8) i	i 225.3 (9.3) M 204.4 (2.5) col 194.4 (6.7) L_{tet}
29−7	29.4	1.05	L 121.2 (10.7) L_{hex} 216.4 (0.9) L_{tet} 245.3 (2.9) col	col 238.1 (2.0) L_{tet} 214.8 (0.8) L_{hex}
32−8	32.2	1.06	L 141.3 (10.4) L_{hex} 242.6 (2.2) L_{tet}	L_{tet} 233.6 (2.5) L_{hex}

[a] L: lamellar, M_{tet}: body-centered tetragonal micelle, col: hexagonal columnar, M: random micelle, L_{tet}: tetragonally perforated lamellar, L_{hex}: hexagonally perforated lamellar, i: isotropic. [b] Determined by NMR Data. [c] Determined by GPC.

scans are summarized in Table 1. To investigate the detailed supramolecular structures of the rod−coil molecules, X-ray scattering experiments were performed at various temperatures. The results of small-angle X-ray diffraction measurements, the molecular densities and the calculated molecular lengths are summarized in Table 2.

As can be observed from Figure 2 and Table 1, **16−4** melts into a birefringent liquid crystalline phase that transforms into an optically isotropic mesophase at 100 °C, followed by isotropic liquid. The small-angle X-ray diffraction pattern of **16−4** in the crystalline phase displays three sharp reflections that correspond to a lamellar structure (Figure 3a). The layer spacing appears to be 8.0 nm that is smaller than the calculated molecular length, indicating that the rod segments are packed into a tilted monolayer lamellar structure. Within the layer, the rod building blocks of the molecule are packed into a rectangular lattice, as confirmed by wide-angle X-ray diffraction patterns. On melting into the birefringent mesophase, the small-angle X-ray diffraction pattern as shown in Figure 3b exhibits a number of sharp peaks that can be indexed as a 3-D body centered tetragonal symmetry with lattice parameters $a = 9.8$ nm and $c = 8.9$ nm ($c/a = 0.91$), whereas the WAXS pattern shows only a broad halo, indicative of liquidlike order of the rod segments within domains. It is worthy of note that the peak corresponding to the 101 and 110 reflections appears to be the most intense in the SAXS pattern, suggesting that the birefringent mesophase of **16−4** is the 3-D tetragonal structure based on discrete bundles. On cooling from the optically isotropic phase, rectangular areas growing in four directions can be observed with a final development of mosaic texture on the polarized optical microscope, characteristics of a tetragonal mesophase exhibited by rod−coil systems.[20,21]
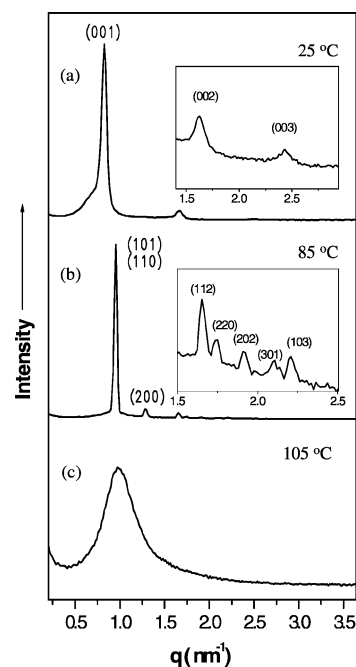
Table 2. Characterization of Rod−Coil Molecules $n-x$ by Small-Angle X-ray Scattering

				crystalline phase										liquid crystalline phase			
				lamellar	3-D hexagonal			3-D tetragonal			hexagonal columnar		body-centered tetragonal		micellar phase	
				lattice constant	lattice constant		perforation diameter	lattice constant		perforation diameter	lattice constant		lattice constant			
molecule	f_{rod}[a]	density ρ (g/cm³)[b]	calculated molecular length (nm)[c]	d_{100} (nm)	a (nm)	c (nm)	d (nm)	a (nm)	c (nm)	d (nm	d_{100} (nm)	a (nm)	a (nm)	c (nm)	primary peak (nm)	diameter (d) (nm)
16−4	0.23	1.056	9.5	8.0									9.8	8.9	6.5	8.0
21−5	0.23	1.057	12.2	8.7				18.4	15.0	12.3	7.5	8.6			6.9	8.5
24−6	0.23	1.062	14.0	9.4				19.9	16.3	14.0	7.9	8.9			7.4	9.0
29−7	0.23	1.064	17.2	10.3	13.2	18.9	11.6	20.6	18.1	15.4	8.5	9.8				
32−8	0.23	1.069	18.8	11.0	16.7	22.6	12.4	24.7	22.1	17.4						

[a] f_{rod} = rod to coil volume ratio. [b] ρ = molecular density. [c] Calculated molecular length = determined from density measurements.
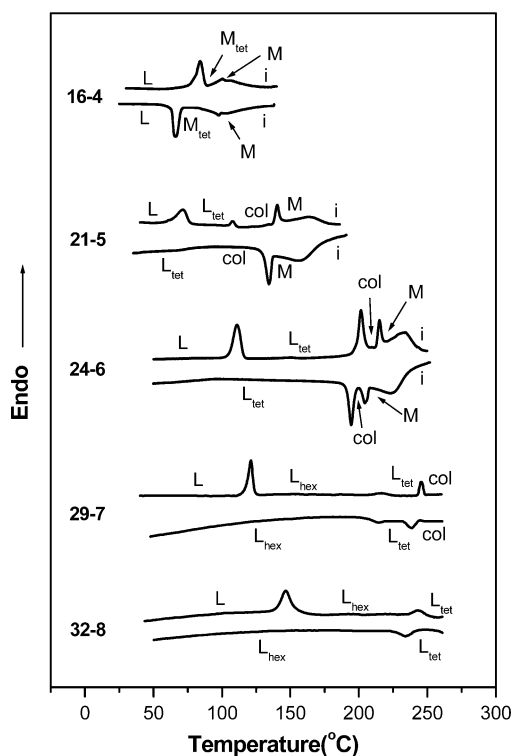
Figure 2. DSC traces (10 °C/min) recorded during the heating scan and the cooling scan by rod−coil molecules $n-x$.

These results together with optical microscopic observations indicate that, on heating, the lamellar structure of **16−4** transforms into discrete bundles that organize into a 3-D body centered tetragonal lattice (Figure 4).[20,21] This indicates that an abrupt structural change from the sheetlike rod domains (1-D lamellar) to discrete bundles (3-D tetragonal) occurs without passing through any intermediate structures such as 2-dimensionally ordered structures and bicontinuous cubic structures. In the optically isotropic mesophase, the SAXS pattern shows only a single strong peak at d-spacing of 6.5 nm (Figure 3c), indicative of a random micellar structure with a diameter of 8.0 nm. These results indicate that, on further heating, the 3-dimensional lattice of the rod-bundles collapses into a disordered micellar structure with only liquidlike short range order of aggregate centers, most probably due to random thermal motion of discrete aggregates.[17c,22]

(22) (a) Sakamoto, M.; Hashimoto, T.; Han, C.-D.; Vaidya, N. Y. *Macromolecules* **1997**, *30*, 1621−1632. (b) Schwab, M.; Stuehn, B. *Phys. Rev. Lett.* **1996**, *76*, 924−927.
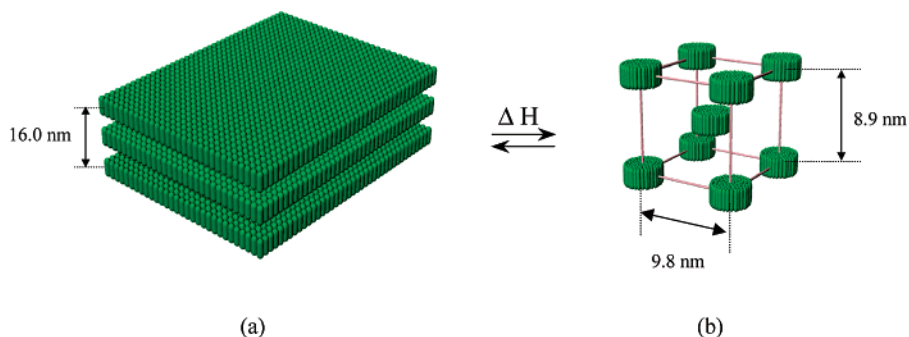
Figure 3. Small-angle X-ray diffraction patterns of **16−4** measured at different temperature plotted against q ($= 4\pi \sin \theta/\lambda$) in (a) the lamellar phase, (b) the bodycentered tetragonal phase and (c) the random micellar phase.

Both **21−5** and **24−6** show multiple phase transitions in the crystalline state, together with an optically isotropic mesophase at higher temperature as confirmed by DSC scans (Figure 2). As confirmed by SAXS scatterings (Figure 5), both the molecules at ambient temperature self-assemble into a lamellar structure with lattice constants of 8.7 and 9.4 nm for **21−5** and **24−6**, respectively. The wide-angle X-ray diffraction patterns of these molecules are similar to that appeared in the crystalline state of **16−4**, indicating that the rod building blocks are crystallized into a rectangular lattice (Figure 6).

With increasing temperature, the small-angle X-ray scattering patterns appear to be a number of well-resolved reflections (Figure 5b), indicating the existence of a highly ordered nanoscopic structure. These reflections can be indexed as a 3-D body centered tetragonal structure with lattice parameters $a = 18.4$ nm, $c = 15.0$ nm for **21−5** and $a = 19.9$ nm, $c = 16.3$ nm for **24−6** (Table 2).[20a,21] It should be noted that the observed X-ray reflections agree well with the expected relative peak positions for a 3-D body centered tetragonal structure, as shown in Table 3. On heating, the tetragonally ordered structure transforms into a 2-D hexagonal columnar structure with lattice constants $a = 8.6$ and 8.9 nm for **21−5** and **24−6**, respectively.

(a) (b)

Figure 4. Schematic representation of self-assembly of **16−4** into (a) 1-D lamellar structure and (b) 3-D tetragonal micellar structure.
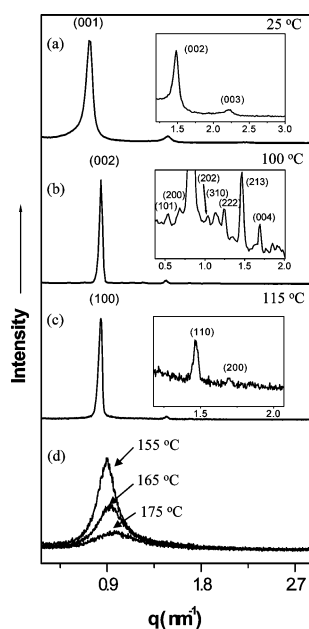

Figure 5. Small-angle X-ray diffraction patterns measured at different temperatures plotted against q (= $4\pi \sin \theta/\lambda$) in (a) the lamellar phase, (b) the tetragonally perforated lamellar phase, (c) the hexagonal columnar phase and (d) the random micellar phase for **21−5**.

Thus, the tetragonal structure in these molecules exists as an intermediate structure between the lamellar and 2-D hexagonal columnar structures. This is in contrast to the thermal behavior of the tetragonal phase exhibited by other rod−coil systems reported previously.[10−21] Another interesting point to be noted is that the peak intensity associated with 002 reflection appears to be the most intense (see Figure 5b), implying that the fundamental structure is lamellar. This is also in opposition to that of the tetragonal structure based on discrete bundles exhibited by **16−4** (Figure 3) and other rod−coil molecules.[20a,21] Taking into account the facts described above and the thermal behavior exhibiting as an intermediate structure between the lamellar and columnar structures,[23−25] this 3-D structure can be best described as a system of tetragonally perforated rod layers stacked in ABAB order. Thus, the coil perforations organize into a 3-D body-centered tetragonal structure. Based on the lattice parameters and the molecular densities, the perforation sizes in diameter are estimated to be 12.3 and 14.0 nm for **21−5** and **24−6**, respectively.

(23) Luzzati, V.; Tardieu, A.; Gulik-Krzwicki, T. *Nature* **1968**, *217*, 1028−1030.
(24) Kekicheff, P.; Tiddy, G. J. T. *J. Phys. Chem.* **1989**, *93*, 2520−2526.
(25) Burger, C.; Micha, M. A.; Oestereich, S.; Föster, S.; Antonietti, M. *Europhys. Lett.* **1998**, *42*, 425−429.
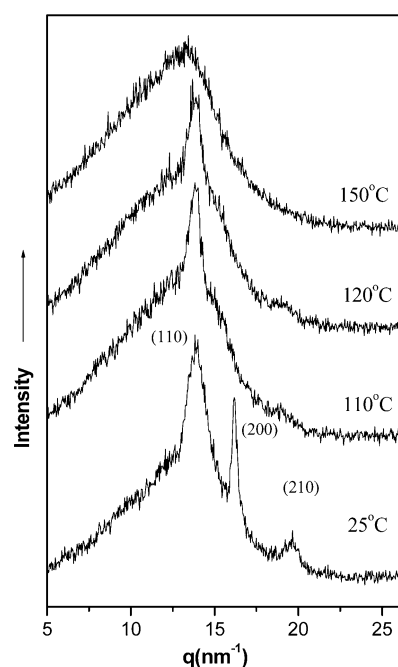
Figure 6. Wide-angle X-ray diffraction patterns measured at various temperatures for **21−5**.

Table 3. Small Angle X-ray Diffraction Data for Tetragonally Perforated Layer Structure of Rod−Coil Molecule **21−5** at 100 °C

h	k	l	q_{obsd} (nm^{-1})	q_{calcd} (nm^{-1})
1	0	1	0.527	0.527
2	0	0	0.691	0.691
0	0	2	0.798	0.798
2	0	2	1.054	1.040
3	1	0	1.089	1.040
3	0	1	1.104	1.139
2	2	2	1.282	1.282
3	1	2	1.367	1.353
4	0	0	1.367	1.353
2	1	3	1.467	1.467
4	1	1	1.467	1.467
0	0	4	1.673	1.696
2	0	4	1.816	1.851

[a] q_{obsd} and q_{calcd} are the scattering vectors of the observed reflections, and calculated for the tetragonally perforated layer structure (*I4/mmm* space group symmetry) with lattice parameters $a = 18.4$ and $c = 15.0$ nm.

Small-angle X-ray diffraction patterns at the optically isotropic phase at high temperature above the hexagonal columnar structure, exhibits only a strong reflection that decreases gradually until the structure changes completely into isotropic liquid, similar to that of **16−4** (Figure 5d). Considering liquidlike micelles, the diameters of sphere can be calculated
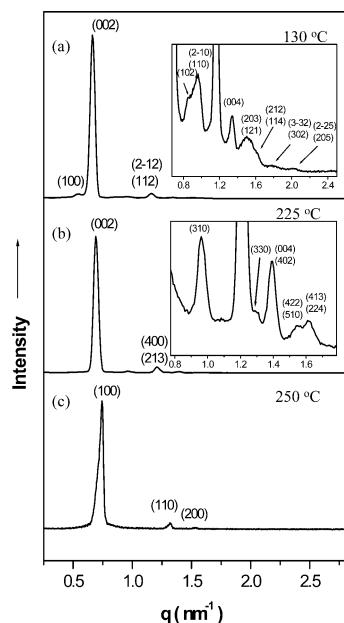
Figure 7. Small-angle X-ray diffraction patterns measured at different temperature plotted against q ($= 4\pi \sin \theta / \lambda$) in (a) the hexagonally perforated lamellar phase, (b) the tetragonally perforated lamellar phase and (c) the 2-D hexagonal columnar phase for **29−7**.

Table 4. Small Angle X-ray Diffraction Data for Hexagonally Perforated Layer Structure of Rod−Coil Molecule **29−7** at 130 °C

h	k	l	q_{obsd} (nm^{-1})	q_{clacd} (nm^{-1})
1	0	0	0.547	0.547
1	0	1	0.664	0.640
0	0	2	0.640	0.640
1	0	2	0.860	0.861
2	−1	0	0.948	0.948
1	1	0	0.948	0.948
2	−1	2	1.157	1.158
1	1	2	1.157	1.158
0	0	4	1.327	1.330
2	0	3	1.480	1.481
3	−1	1	1.486	1.486
1	2	1	1.486	1.486
3	−1	2	1.593	1.594
2	1	2	1.593	1.594
2	−1	4	1.631	1.633
1	1	4	1.631	1.633
3	−3	2	1.772	1.772
2	−2	5	1.999	2.001
2	0	5	1.999	2.001

[a] q_{obsd} and q_{calcd} are the scattering vectors of the observed reflections, and calculated for the hexagonally perforated layer structure ($P6_3/mmc$ space symmetry) with lattice parameters $a = 13.2$ and $c = 18.9$ nm.
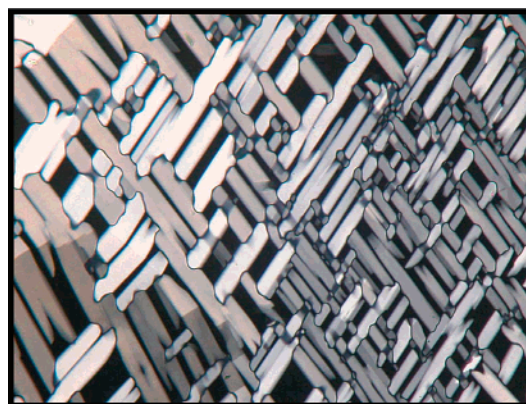

Figure 8. Representative optical polarized micrograph (100×) of the texture exhibited by the tetragonally perforated lamellar phase of **29−7** at 225 °C on cooling scan.

to be 8.5 and 9.0 nm for **21−5** and **24−6**, respectively.[17c,22] These results indicate that the 2-D hexagonal columnar structure transform, on heating, into a discrete micellar structure with a lack of 3-D symmetry. This behavior can be rationalized by considering the coil segments to be conformationally flexible. On heating, higher thermal motion of flexible coils relative that of the stiff-rod segments leads to more curling of coils, consequently requiring larger interfacial area. This spatial requirement results in the split of the extended columns into discrete bundles. The tendency of the lamellar or columnar structures to split into smaller domains on heating is consistent with the results described previously.[17c,19a,20a,21]

On further increment in the molecular length, the interesting phase behavior can be observed. Similar to the molecules described above, both **29−7** and **32−8** also self-assemble, at first, into a lamellar structure, in which rod building blocks are crystallized into a rectangular lattice within aromatic domains. On heating, however, the lamellar structure of both the molecules transforms into a perforated layered structure with a 3-D hexagonal lattice rather than a tetragonal lattice. The small-angle X-ray diffraction pattern of **29−7** displays a number of sharp peaks, which can be indexed as a 3-D hexagonal order ($P6_3/mmc$ space group symmetry) with lattice parameters $a = 13.2$ nm and $c = 18.9$ nm (Figure 7a and Table 4).[20a,21]

Interestingly, the heating DSC curve of **29−7**, as shown in Figure 2, shows to be an additional phase transition at 216 °C, suggesting that the presence of the intermediate structure between the hexagonally perforated lamellar and columnar phases. The small-angle X-ray diffraction pattern taken at 225 °C shows several reflections corresponding to a 3-D body centered tetragonal lattice with a lattice parameters $a = 20.6$ nm and $c = 18.1$ nm (Figure 7b). On cooling from the optically isotropic phase and then annealing at 230 °C, the formation of rodlike domains growing in two different directions which merge into a 2-dimensional network texture could be observed on the polarized optical microscope, further supporting the existence

of a tetragonal order. Figure 8 shows a representative texture of the tetragonal phase exhibited by **29−7** on cooling scan. Taking into account the presence of the very strong 002 reflection in the small-angle X-ray diffraction pattern and its position in the phase sequence, located between lamellar and columnar phases, the 3-D tetragonal structure can be considered as a perforated lamellar structure in analogy with **24−6**.

These results together with the DSC scans indicate that the 3-D symmetry change, from a hexagonal- to a tetragonal lattice in the perforated layered structure, occurs in a reversible way by changing temperature. Figure 9 illustrates the possible models responsible for the transformation between the hexagonally perforated and tetragonally perforated lamellar structures depending on temperature. In comparison with the phase behavior of **24−6**, this indicates that increasing the rod length leads to the formation of a perforated layer with a 3-D hexagonal lattice, whereas reduction in its length favors a perforated layer with a 3-D tetragonal lattice.

Discussion

At ambient temperature, all the rod−coil molecules assemble into a lamellar structure, in which the rod building blocks
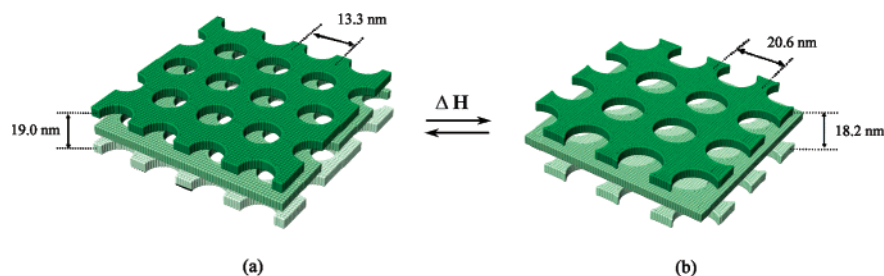
Figure 9. Schematic representation of self-assembly of **29−7** into a perforated lamellar structure with (a) 3-D hexagonal lattice and (b) 3-D tetragonal lattice.
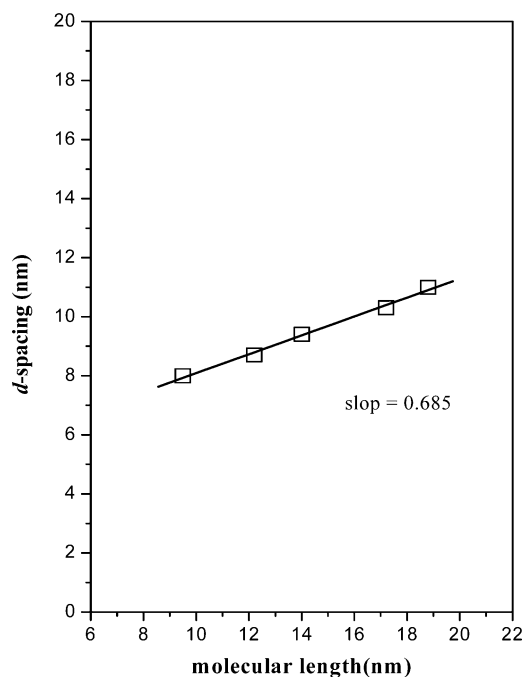

Figure 10. Dependence of *d*-spacing of the rod−coil molecule *n−x* in the lamellar crystalline phase on the molecular length.

crystallize into a rectangular lattice within aromatic domains. Figure 10 shows the dependence of *d*-spacing of the lamellar structure as a function of the calculated molecular length of the rod−coil molecule. As shown in Table 2, the *d*-spacing systematically increases with the calculated molecular length. The value, however, is smaller than the corresponding molecular length in each of the molecules, indicative of a rod tilt with respect to the interface separating the rod and coil domains. Notably, the slope is less than unity, implying that the extent of the rod tilt increases with increasing the molecular length.[17b] This behavior can be rationalized by considering the energetic penalties associated with deformation of coil segments, as well illustrated by rod−coil theories.[26−31]

In contrast, significant supramolecular structural change at elevated temperature is observed as the molecular length is varied at an identical rod to coil volume ratio. The experimental results described here demonstrate that the systematic elongation of the rod segment leads to a structural transformation from a

discrete bundle structure via a variety of intermediate structures including 3-D perforated lamellar and 2-D columnar structures to a lamellar structure. This interesting variation in the supramolecular structure, at an identical rod-to-coil volume ratio can be explained by considering the tendency of the rod building block to be arranged with their long axes.[26−31] On increasing the rod length, attractive interactions between the rod segments would be greater, which results in the organized structures with successive decrease in the interfacial area.

The **16−4** based on a short rod length shows a 3-D discrete structure above a lamellar crystalline structure, most probably due to the relatively large entropic contribution to the free energy associated with a short molecular length. On elongation of the rod building blocks, the strong tendency of the rods to be aligned axially with their long axes makes a greater enthalpic contribution to the free energy balance at the expense of entropic penalties associated with coil stretching. Accordingly, the discrete domains would merge into a larger domain as in the case of **21−5** and **24−6** that self-assemble into infinitely long strips and tetragonally perforated layers, to reduce interfacial energy associated with unfavorable segmental contacts. Remarkably, further increasing the rod length gives rise to a hexagonally perforated layered structure as in the case of **29−7** and **32−8**. In addition, the hexagonal symmetry of the perforations in these molecules transforms to a tetragonal arrangement reversibly by changing temperature in these molecules, as illustrated in Figure 9. Therefore, changing temperature produces an effect similar to varying the molecular length. These results demonstrate that systematic variation of the rod length at an identical rod to coil volume fraction can provide a strategy to regulate the organized structure, from discrete bundles, long strips, perforated layers with both tetragonal and hexagonal symmetries to conventional layers.

Compared to other self-assembling systems including block copolymers,[3,4,25,32,33] liquid crystals[2], and surfactant systems,[23,24,34] the unique feature of the structurally simple rod−coil diblock systems described here is their ability to self-assemble into stable perforated lamellar structures having different 3-D lattices with a small variation in the rod length. Furthermore, the 3-D symmetry of the coil perforation changes directly from a tetragonal to a hexagonal lattice in a reversible way with variation in temperature as in the case of **29−7** and **32−8**. This transition may arise from the fact that, with

(26) Matsen, M. W.; Bates, F. S. *Macromolecules* **1996**, *29*, 1091−1098.
(27) Müller, M.; Schick. M. *Macromolecules* **1996**, *29*, 8900−8903.
(28) Halperin, A. *Macromolecules* **1990**, *23*, 2724−2731.
(29) Semenov. A. N. *Mol. Cryst. Liq. Cryst.* **1991**, *209*, 191−200.
(30) Williams, D. R. M.; Fredrickson, G. H. *Macromolecules* **1992**, *25*, 3561−3568.
(31) Raphael. E.; de Genn, P. G. *Makromol. Chem., Macromol. Symp.* **1992**, *62*, 1−16.

(32) Ahn, J.-H.; Zin, W.-C. *Macromolecules* **2000**, *33*, 641−644.
(33) Raez, J.; Tomba, J. P.; Manners, I.; Winnik, M. A. *J. Am. Chem. Soc.* **2003**, *125*, 9546−9547.
(34) Fairhurst, C. E.; Fuller, S.; Gray, J.; Holmes, M. C.; Tiddy, G. J. T. *Handbook of Liquid Crystals*; Demus, D., Goodby, J., Gray, G. W., Spiess, H.-W., Vill, V., Eds.; Wiley-VCH: Weinheim, Germany, 1998; Vol. 3, p 341.

increasing the rod length or lowering temperature, packing arrangement of coil perforations has a tendency to pack more densely. Consequently, the 3-D tetragonal lattice of coil perforations transforms into a 3-D hexagonal lattice that allows more close packing.

Conclusions

Rod−coil diblock molecules with variation in the rod length, but identical rod to coil volume ratio were synthesized and characterized, and their self-assembling behavior was investigated by using DSC and X-ray scatterings. These molecules were observed to self-assemble into aggregate structures that differ significantly as a function of the molecular length. The molecule with a short rod−coil molecule containing two biphenyl units as the rod segment (**16**−**4**) shows a 3-D tetragonal structure based on a body-centered symmetry of the discrete bundles in addition to a lamellar structure. This 3-D lattice, on heating, collapses to generate a disordered micellar structure. Remarkably, the molecules based on longer rod segments (**21**−**5** and **24**−**6**) were observed to self-organize into multiple supramolecular structures accessible through a change in temperature. The molecules show, on heating, lamellar, tetagonally perforated lamellar, 2-D hexagonal columnar and finally disordered micellar structures. Further increase in the molecular length as in the case of **29**−**7** and **32**−**8** induces a 3-D hexagonally perforated lamellar structure as an intermediate structure between the lamellar and tetragonally perforated lamellar structures. Consequently, these systems clearly demonstrate the ability to regulate the domain nanostructure, from 2-dimensionally continuous layers, long strips to discrete bundles via periodic perforated layers by small changes in the rod length, at an identical rod-to-coil volume fraction. It is worthy of note that the perforated lamellar structures are equilibrium structures and thus, the 3-D lattice of the perforations can also be manipulated by a change in the rod length in a reversible way. The work described here suggests that this approach to regulating supramolecular structure will lead to a wide range of functional materials with tunable nanoscopic properties and potentially interesting applications such as periodic porous materials, nanopatterning, and nanostructured templates.

Supporting Information Available: Experimental details (PDF). This material is available free of charge via the Internet at http://pubs.acs.org.

JA039793Q